Forces in Motzkin paths in a wedge

2006 J. Phys. A: Math. Gen. 39 1581

(http://iopscience.iop.org/0305-4470/39/7/005)

INSTITUTE OF PHYSICS PUBLISHING JOURNAL OF PHYSICS A: MATHEMATICAL AND GENERAL

J. Phys. A: Math. Gen. **39** (2006) 1581–1608 doi:10.1088/0305-4470/39/7/005

Forces in Motzkin paths in a wedge

E J Janse van Rensburg

Department of Mathematics and Statistics, York University, 4700 Keele Street, Toronto, Ontario, M3J 1P3, Canada

E-mail: rensburg@yorku.ca

Received 5 October 2005, in final form 30 November 2005
Published 1 February 2006
Online at stacks.iop.org/JPhysA/39/1581

Abstract

Entropic forces in models of Motzkin paths in a wedge geometry are considered as models of forces in polymers in confined geometries. A Motzkin path in the square lattice is a path from the origin to a point in the line $Y = X$ while it never visits sites below this line, and it is constrained to give unit length steps only in the north and east directions and steps of length $\sqrt{2}$ in the north-east direction. Motzkin path models may be generalized to ensembles of NE-oriented paths above the line $Y = rX$, where $r > 0$ is an irrational number. These are paths giving east, north and north-east steps from the origin in the square lattice, and confined to the r-wedge formed by the Y-axis and the line $Y = rX$. The generating function g_r of these paths is not known, but if $r > 1$, then I determine its radius of convergence to be

$$t_r = \min_{\frac{r-1}{r} \leqslant y \leqslant \frac{r}{r+1}} [y^y (1 - r(1-y))^{1-r(1-y)} (r(1-y) - y)^{r(1-y)-y}],$$

and if $r \in (0, 1)$, then $t_r = 1/3$. The entropic force the path exerts on the line $Y = rX$ may be computed from this. An asymptotic expression for the force for large values of r is given by

$$F(r) = \frac{\log(2r)}{r^2} - \frac{1 + 2\log(2r)}{2r^3} + O\left(\frac{\log(2r)}{r^4}\right).$$

In terms of the vertex angle α of the r-wedge, the moment of the force about the origin has leading terms

$$F(\alpha) = \log(2/\alpha) - (\alpha/2)(1 + 2\log(2/\alpha)) + O(\alpha^2 \log(2/\alpha))$$

as $\alpha \to 0^+$ and $F(\alpha) = 0$ if $\alpha \in [\pi/4, \pi/2]$. Moreover, numerical integration of the force shows that the total work done by closing the wedge is 1.085 07 . . . lattice units. An alternative ensemble of NE-oriented paths may be defined by slightly changing the generating function g_r. In this model, it is possible to determine closed-form expressions for the limiting free energy and the force. The leading term in an asymptotic expansions for this force agrees with the leading term in the asymptotic expansion of the above model, and the subleading term only differs by a factor of 2.

PACS numbers: 05.50.+q, 02.10.Ab, 05.40.Fb, 82.35.−x

1. Introduction

Models of lattice paths have been used for decades to study the physical properties of polymers in solution [3, 6, 7]. These models, which include the self-avoiding walk and a variety of directed lattice path and vesicle models, are now an integral part of standard statistical mechanics and combinatorics literature. The models pose challenging mathematical questions, involving techniques from analysis, combinatorics, statistical mechanics and asymptotic analysis, and so they remain the focus of intensive investigation.

The self-avoiding walk model remains unsolved, although significant progress has been made in the study of its scaling limits and other properties [6, 7, 9, 26]. Self-avoiding walks in confined geometries have also been studied [10, 11, 22–25], for a more recent reference see [8]. The connection between some of these models and conformal field theories has considerably advanced the understanding of the self-avoiding walk in wedge geometries, and there are predicted exact values for some critical exponents in the literature [5, 19].

Fully directed and partially directed path models of linear polymers are Markovian in nature and may be exactly solvable. In these models the scaling properties can be examined explicitly and inform us of the scaling of thermodynamic quantities of the self-avoiding walk or even of linear polymers in solution. There is a large literature devoted to directed path models, and much progress have been made solving for the generating functions and other properties of these models [1, 20, 21], see also [12] and the citations therein.

Directed and partially directed lattice path models of linear polymers in confined geometries have also been studied, and in figure 1 an example of a directed path confined to a wedge is illustrated. Brak *et al* [2] considered a directed path in a slit as a model of a polymer between two confining planes, see also [16] for simulations of a self-avoiding walk between confining planes. This model is a generalization of a model of a directed path adsorbing on a wall [1], and the polymer exerts a repulsive entropic force on the confining planes. This repulsive force is the essential ingredient in steric stabilization of colloid dispersions. A loss of entropy in adsorbed polymer chains as particles approach one another results in a repulsive force between the particles [17].

Self-avoiding walk models of polymers in wedge geometries have been considered in the literature [5, 19], and a model of generalized Dyck words studied in [4] corresponds to a model of directed paths in a wedge. Directed and partially directed paths in wedge geometries were also considered in [13, 14]. In these papers models of adsorbing directed and partially directed paths are examined and the location of the adsorption critical point is approximated.

Forces in a model of fully directed paths in a wedge (see figure 1) were examined in [15]. The path exerts an extropic force on the wedge, and the moment of this force about the origin is a function of the vertex angle α of the wedge. This moment has magnitude

$$F_\alpha = \begin{cases} \left[\dfrac{1+\cot^2\alpha}{(1+\cot\alpha)^2}\right]\log\cot\alpha & \text{if} \quad \alpha \in [0, \pi/4], \\ 0 & \text{if} \quad \alpha \in [\pi/4, \pi/2], \end{cases} \tag{1}$$

and it vanishes at $\alpha = \pi/4$; for larger angles the moment is identically zero. The entropic contribution of the path to the force is non-zero only for vertex angles smaller than $\pi/4$.

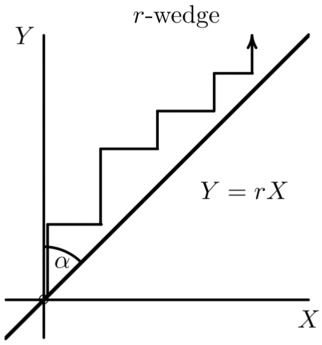

Figure 1. A fully directed path in a wedge formed by the Y-axis and the line $Y = rX$, where $r > 0$ is a real number. The path exerts a repulsive entropic force on the lines bounding the wedge—if the angle has a rational tangent. If the tangent is not rational, then the line never visits points in the line, but may come arbitrarily close. The magnitude of the force is given by equation (1).

In contrast, the free energy of a self-avoiding walk in a wedge does not contain a angle-dependent component in the scaling limit [10], and so there is no entropic component in the force. Thus, the interaction of the walk with the wedge boundaries does not contain an entropic component. A directed path in a wedge is also related to a model of a directed path in a slit [2], and an explicit expression for the repulsive entropic force between the confining lines of the slit has been determined in that model as well.

In this paper, I generalize the results in [15] to models of Motzkin paths in a wedge. Section 2 is a short overview of the generating function and properties of Motzkin paths. I introduce *NE-oriented paths* from the origin in the square lattice. These are paths which may step in the east (E) or north (N) directions in unit length steps, but which can also step in the north-east (NE) directions in a step of length $\sqrt{2}$. An NE-oriented path is illustrated in figure 2(a).

Motzkin paths are NE-oriented paths that may step only on vertices above or on the line $Y = X$ and with final vertex in the line $Y = X$. A Motzkin path is illustrated in figure 2(b). If t is the generating variable of edges in Motzkin paths, and the generating function of Motzkin paths is $g_1 \equiv g_1(t)$, then it is known that g_1 satisfies the recurrence

$$g_1 = 1 + tg_1 + t^2 g_1^2. \tag{2}$$

Motzkin paths are briefly reviewed in section 2.

The definition of a Motzkin path may be broadened to include paths in more general wedges. Consider, for example, the pair of relative prime integers (p, q). The (q/p)-wedge formed by the line $Y = (q/p)X$ and the Y-axis may contain an NE-oriented path with final vertex in the line $Y = (q/p)X$. Such a path is illustrated in figure 2(c) and it is a (q/p)-*Motzkin path*.

In the event that $p = 1$ the q-wedge is formed by the line $Y = qX$ and the Y-axis. In this case, a model of NE-oriented paths in the q-wedge with final vertex in the line $Y = qX$ is obtained. These are q-Motzkin paths. In section 3, the results in section 2 are generalized to a q-Motzkin paths. I show that the generating function $g_q \equiv g_q(t)$ of the q-Motzkin paths satisfy the polynomial

$$t^{q+1} g_q^{q+1} + t^q g_q^q - g_q + 1 = 0. \tag{3}$$

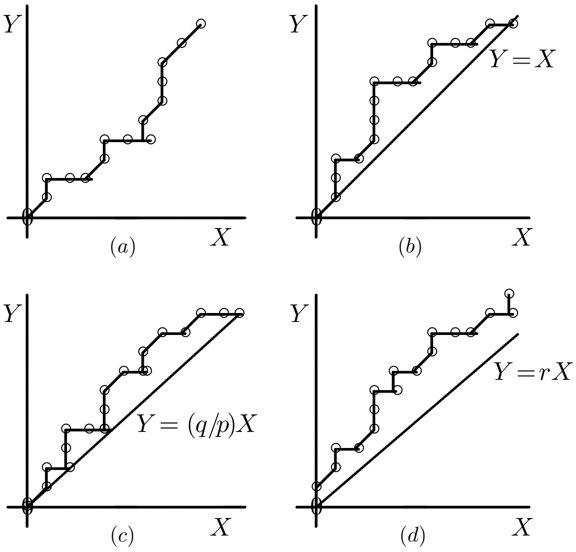

Figure 2. (*a*) An NE-oriented path. The path takes steps in the north, east and north-east directions only. The length of an NE-oriented path is the number of steps it gives; in this example the length of the path is 14. Observe that steps in the north and east directions have length 1, but that a step in the north-east direction has length $\sqrt{2}$. (*b*) A Motzkin path. The path is an NE-oriented path constrained to start at the origin, to avoid vertices below the line $Y = X$, and to end in a vertex in the line $Y = X$. The length of this Motzkin path is 16. (*c*) A (q/p)-Motkzin path in the (q/p)-wedge defined by the line $Y = (q/p)X$ and the Y-axis. If $p = 1$, then a q-Motzkin path is obtained. (*d*) An r-Motzkin path in the r-wedge defined by the line $Y = rX$ and the Y-axis. Since $r > 0$ is irrational, the path cannot visit vertices in the line $Y = rX$ and its endpoint is not in this line as well.

The generating function of 2-Motzkin paths satisfies a cubic and is determined completely in this section. I also show that g_q is finite for integer q at $t = t_q$ (thus, at its radius of convergence) and that $g_q(t_q) = g^*$ satisfies the polynomial

$$((q-1)g^* - q)^q + (1 + q(1 - g^*))^{q+1} = 0. \tag{4}$$

I also determine an asymptotic expansion for g^*, so that

$$g^* = g_q(t_q) \approx 2 - \sqrt{1 - 2/q}. \tag{5}$$

Numerical comparisons show that this approximation is very accurate, even for small values of q.

Lastly, one may further extend the definition of Motzkin paths to NE-oriented paths confined in an arbitrary wedge. Let $r > 0$ be an irrational number and consider the r-wedge defined by the Y-axis and the line $Y = rX$. An r-Motzkin path is an NE-oriented path from the origin confined to the r-wedge. Observe that for irrational r the endpoint of the path cannot be in the line $Y = rX$, but is somewhere else in the r-wedge. The generating function $g_r \equiv g_r(t)$ of r-Motzkin paths is defined by

$$g_r = \sum_{n \geqslant 0} c_n(r) t^n, \tag{6}$$

where $c_n(r)$ is the number of NE-oriented paths of length n steps and confined to the r-wedge (these are r-Motzkin paths). Observe that if $r = q/p$ is rational, then one may consider $g_{q/p}$

as the generating function of (q/p)-Motzkin paths with final vertex in the line $Y = (q/p)X$. An r-Motzkin path is illustrated in figure 2(d).

In section 4, I prove that

$$\lim_{n\to\infty}[c_n(r)]^{1/n} = \Big[\inf_{p_x,p_y} p_x^{p_x} p_y^{p_y}(1-p_x-p_y)^{1-p_x-p_y}\Big]^{-1} \tag{7}$$

where the infimum is taken subject to $0 \leqslant p_x + p_y \leqslant 1$ and $(1-p_x) = r(1-p_y)$. This result implies that the radius of convergence of $g_r(t)$ is given by

$$t_r = \begin{cases} \frac{1}{3}, & \text{if} \quad r \in [0,1], \\ \inf_{p_x,p_y}\left[p_x^{p_x} p_y^{p_y}(1-p_x-p_y)^{1-p_x-p_y}\right], & \text{if} \quad r \in (1,\infty), \end{cases} \tag{8}$$

where the infimum is taken subject to $0 \leqslant p_x + p_y \leqslant 1$ and $(1-p_x) = r(1-p_y)$. Since this is an infimum over a compact domain, it can be replaced by a minimum, and this proves the claim in the abstract.

The results in section 4 make it possible to compute asymptotic approximations to the forces of the r-Motzkin path on the r-wedge. This is done in section 5, and the force along the line $X = 1$ has magnitude

$$F(r) = \frac{\log(2r)}{r^2} - \frac{1+2\log(2r)}{2r^3} + O\left(\frac{\log(2r)}{r^4}\right) \tag{9}$$

and it works against the closing of the wedge. Numerical solutions of the model show that this expression becomes very accurate for $r > 10$. The moment of this force about the origin has asymptotic approximation

$$F(\alpha) = \log(2/\alpha) - (\alpha/2)(1+2\log(2/\alpha)) + O(\alpha^2\log(2/\alpha)). \tag{10}$$

Observe that the logarithm diverges as $\alpha \to 0^+$. For fully directed paths the similar expression $F_\alpha = -\log\alpha + 2\alpha\log\alpha + \cdots$ was obtained in [15], and this shows the same logarithmic divergence as the wedge angle approaches zero. The total work done by closing the r-wedge from an angle larger than $\pi/4$ may also be determined by integrating the force. In this model, this amount is 1.08507... lattice units of work. In contrast, closing a wedge on a self-avoiding walk would require no work [10].

It is not possible to solve explicitly for the radius of convergence of g_r. Thus, explicit solutions for the forces in this model remain unknown, but I have been able to determine asymptotic expansions approximating these well in the large r-limit. An alternative model may be defined by counting NE-oriented paths by their *span*: an NE-oriented path from the origin to the vertex (X, Y) will have span $X + Y$, but length (number of steps) at most $X + Y$ and at least $|X - Y| + \min\{X, Y\}$. Let $m_r(n)$ be the number of NE-oriented paths of span n in the r-wedge defined by the Y-axis and the line $Y = rX$. Consider the generating function

$$h_r = \sum_{n\geqslant 0} m_r(n)t^n. \tag{11}$$

In the first model, edges were generated by t in the generating function g_r. In this model, t is the generating variable for span in h_r. One may interpret t as a length or step-generating variable by noting that N- and E-edges would be weighted by t each in this ensemble, but diagonal edges or NE-step would be weighted by t^2.

In section 6, the model defined by h_r is examined. I determine an explicit expression for the radius of convergence of h_r. The result is that the entropic force acting on the wedge can be determined in closed form. While these expressions are lengthy, it is possible to determine

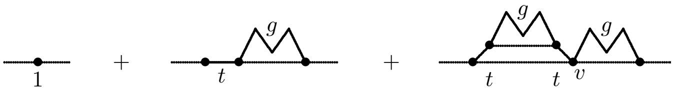

Figure 3. Each Motzkin path is either (1) the empty path or (2) first steps in the NE-direction and then continues as an arbitrary Motzkin path or (3) first steps in the N-direction and returns for a first time to the line $Y = X$ at the vertex v, thereafter it continues as an arbitrary Motzkin path. The line $Y = X$ is oriented horizontally in this schematic figure.

asymptotic expansions for the free energy and the forces. The magnitude of the force along the line $X = 1$ has asymptotic approximation in r given by

$$F(r) = \frac{\log(2r)}{r^2} - \frac{1 + 2\log(2r)}{r^3} + O\left(\frac{\log(2r)}{r^4}\right). \tag{12}$$

This expression differs from equation (9) by a factor of 2 in the denominator of the subleading term. The moment of the force about the origin is similarly given in terms of the vertex angle α of the r-wedge by

$$F(\alpha) = \log(2/\alpha) - \alpha(1 + 2\log(2/\alpha)) + O(\alpha^2 \log(2/\alpha)). \tag{13}$$

The total work done by closing the r-wedge from an angle larger than $\pi/4$ in this model may be calculated to be 0.881 3735 ... lattice units of work.

The paper is concluded by a few final comments and observations in section 7.

2. Motkzin paths in a wedge

The number of NE-oriented paths with n east steps, m north steps and s NE-steps is the trinomial coefficient (these are multinomial coefficients $C(n, n_1, n_2, \ldots, n_k)$ with $k = 3$)

$$\binom{n+m+s}{n, m, s} = \frac{(n+m+s)!}{n!m!s!}. \tag{14}$$

Observe that such paths have length $n + m + s$ (measured as the number of edges in the path) and that these paths terminate in the vertex with coordinates $(n + s, m + s)$ if it starts from the origin.

The number of Motzkin paths can be determined by using a generating function technique. Suppose that t is the edge-generating variable of Motzkin paths and that $g_1 \equiv g_1(t)$ is the generating function of Motzkin paths. g_1 can be determined by noting that each Motzkin path is (1) either the empty path consisting of one vertex at the origin or (2) gives a first step in the NE-direction, and then continues as an arbitrary Motzkin path or (3) it steps in the N-direction first and then returns for a first time to the line $Y = X$ at a vertex v, thereafter it continues as an arbitrary Motzkin path. These classes are illustrated in figure 3.

The classification of Motzkin paths in figure 3 gives a recurrence for the generating function g_1 as follows: the empty path is generated by 1. Paths with first step in the NE-direction are generated by tg_1; the extra factor of t accounts for the first step, and g_1 accounts for any arbitrary Motzkin path following this step. Lastly, paths which steps first in the N-direction and then return for a first time to the line $Y = X$ at a vertex v are analysed as follows: first a factor of t for the first N-step. The path then continues as an arbitrary Motzkin path above the line $Y = X + 1$; this is generated by g_1. Finally, the path steps in an E-step into the line $Y = X$ at vertex v, this step is generated by t. Thereafter it continues as an arbitrary Motzkin path above the line $Y = X$ (generated by g_1). Taking together all these factors shows that these paths are generated by $t^2 g_1^2$.

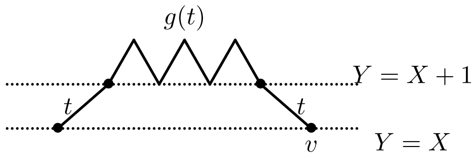

Figure 4. A primitive Motzkin path steps first in the N-direction and then continues as an arbitrary Motzkin path above the line $Y = X + 1$ before it finally steps in the E-direction to terminate in the line $Y = X$. These paths visit the line $Y = X$ only in its terminal (first and last) vertices. It returns for a first time to the line $Y = X$ at v, its final vertex. Since the first and last steps are generated by t and the path is an arbitrary Motzkin path above the line $Y = X + 1$ from its second step until its second last step, primitive paths are generated by $t^2 g_1$.

These arguments are simplified if the notion of a *primitive* Motzkin path is introduced. A Motzkin path is primitive or is an *excursion* if it does not visit the line $Y = X$, except in its first and last vertices. A primitive Motzkin path is schematically illustrated in figure 4. A primitive Motzkin path consists of an N-step, followed by an arbitrary Motzkin path above the line $Y = X + 1$ and then by an E-step. Since arbitrary Motzkin paths are generated by g_1, it follows that primitive Motzkin paths are generated by $t^2 g_1$. Thus, the third class of paths in figure 3 is composed of a primitive Motzkin path followed by an arbitrary Motzkin path at the vertex v.

These ideas make it possible to write a functional recurrence for Motzkin paths. From figure 3 it follows that every Motzkin path is either the empty path or is a north-east step followed by an arbitrary Motzkin path or is composed of a primitive Motzkin path followed by an arbitrary Motzkin path. In other words, g_1 satisfies the recurrence $g_1 = 1 + t g_1 + t^2 g_1^2$ in equation (2). By finding the roots of this polynomial, it follows that the solution for g_1 is the algebraic function

$$g_1 = \frac{1 - t - \sqrt{1 - 2t - 3t^2}}{2t^2}. \tag{15}$$

This root was selected because its expansion as a power series in t gives terms with non-negative coefficients.

The radius of convergence of g_1 can be determined by examining the radical in equation (15). Since $1 - 2t - 3t^2 = (1 - 3t)(1 + t)$, it follows that $t_1 = 1/3$ is the radius of convergence of $g_1(t)$ and we also note that $g_1(t_1) = 3$.

3. q-Motzkin paths

A q-Motzkin path is *primitive* if it is disjoint with vertices in the line $Y = qX$, except for its first and last vertices. The path in figure 5(a) is primitive. Let g_q be the generating function of q-Motzkin paths. Then g_1 is given by equation (15).

The generating function of primitive q-Motzkin paths can be determined by noting that there are two classes of such paths: every primitive q-Motzkin path steps into its last vertex either in an edge which is oriented east or steps into its last vertex in an edge which is diagonally oriented in the north-east direction (see figure 6).

Consider these two classes of primitive q-Motzkin paths separately. In the first class, the last edge is oriented horizontally. Each primitive q-Motzkin path in this class starts at the origin and steps north to the vertex $(0, 1)$. It then continues as an arbitrary q-Motzkin path (generated by g_q) on or above the line $Y = qX + 1$ until it finds its last vertex in this line. It then must step north to a vertex in the line $Y = qX + 2$ and it then continues as an arbitrary

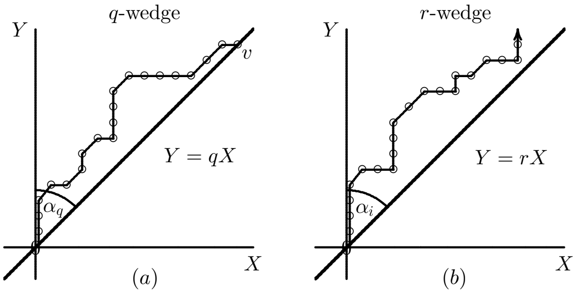

Figure 5. q-Motzkin paths in q-wedges: (a) if q is a positive integer then a q-Motzkin path is an NE-oriented path from the origin in the q-wedge formed by the Y-axis and the line $Y = qX$, terminating in a vertex v in the line $Y = qX$. The coordinates of v is of the form (n, nq), where $n \geqslant 0$ is an integer. (b) If r is an irrational number then the r-Motzkin path is an NE-oriented path from the origin in the r-wedge formed by the Y-axis and the line $Y = rX$. An r-Motzkin path will never intersect the line $Y = rX$ if r is irrational, but will approach it arbitrarily closely.

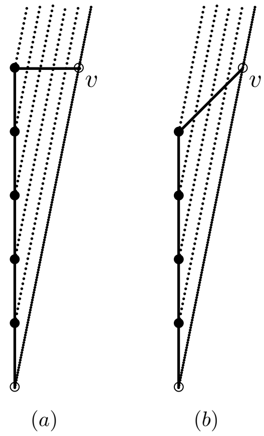

Figure 6. There are two classes of primitive q-Motzkin paths. These can be generated by considering the two shortest q-Motzkin paths ending in the vertex v with coordinates $(1, q)$ (in this diagram, $q = 5$). (a) The first class of primitive q-Motzkin paths is generated from the shortest q-Motzkin path that steps in an east step into its terminal vertex v. Primitive q-Motzkin paths in this class are now generated by first stepping north from the origin. The path may then continue as an arbitrary q-Motzkin path above the line $Y = qX + 1$, until it visits a last vertex in this line. Thereafter it must step north again to a vertex in the line $Y = qX + 2$. It may then continue as an arbitrary q-Motzkin path above the line $Y = qX + 2$, until it finds its last vertex in this line. It then steps north to the line $Y = qX + 3$ and continues from there. Finally, it finds its last vertex in the line $Y = qX + q$ from where it steps horizontally to its terminal vertex v in the line $Y = qX$. This process can be implemented by replacing each vertex marked by a $\bullet$ above by the generating function g_q of q-Motzkin paths. (b) The second class of primitive q-Motzkin paths is generated from the shortest q-Motzkin path that steps in a north-east step into its terminal vertex v. The argument then continues as in (a), except that the path steps to its terminal vertex v in a north-east step from a last visit in the line $Y = qX + q - 1$.

q-Motzkin path until its last visit to this line. Thereafter it steps north again, and at the mth step it is an arbitrary q-Motzkin path above the line $Y = qX + m$, where $1 \leqslant m \leqslant q - 1$. Finally, it visits the line $Y = qX + q - 1$ a last time and it steps north to continue as an arbitrary q-Motzkin path above the line $Y = qX + q$. It visits this line in a final vertex, and then it must step horizontally into the line $Y = qX$ and terminates, since it is primitive. Since m can take $q - 1$ values, and there is one final arbitrary q-Motzkin path above the line $Y = qX + q$, it follows that primitive q-Motzkin paths in the first class are generated by $t^{q+1} g_q^q$. One can also find this by replacing each bullet in figure 6 by a g_q.

The second class of primitive q-Motzkin paths can be generated in the same way as above, visiting the lines $Y = qX + m$ for $m = 1, 2, \ldots, q - 1$ a last time in each case. Finally, when $m = q - 1$, these paths step diagonally north-east (instead of north) into the line $Y = qX$ to terminate, since they are primitive. Accounting in this case shows that primitive q-Motzkin paths in this class are generated by $t^q g_q^{q-1}$. One may also show this by replacing each bullet in figure 6 by a g_q.

Thus, primitive q-Motzkin paths are generated by $t^{q+1} g_q^q + t^q g_q^{q-1}$. To find the recurrence for g_q, observe that each q-Motzkin path is either a single vertex or is a primitive q-Motzkin path followed by an arbitrary q-Motzkin path. In other words,

$$g_q = 1 + \left(t^{q+1} g_q^q + t^q g_q^{q-1}\right) g_q = 1 + t^q g_q^q + t^{q+1} g_q^{q+1}. \tag{16}$$

This is valid if $q \geqslant 1$ and q is an integer. This recurrence is a polynomial in g_q and its roots can be determined for small values of q. Putting $q = 1$ gives the recurrence in equation (2) for the generating function of Motzkin paths. Putting $q = 2$ gives 2-Motzkin paths. A full solution for this model is given next.

3.1. 2-Motzkin paths

Put $q = 2$ in equation (16), then the generating function of 2-Motzkin paths satisfies the cubic polynomial

$$t^3 g_2^3 + t^2 g_2^2 - g_2 + 1 = 0. \tag{17}$$

One may solve explicitly for g_2; and by selecting the appropriate root,

$$\begin{aligned} g_2(t) = &-\frac{1}{3t} - \frac{1+\sqrt{-3}}{12t^2}\left(t^2\left[12\sqrt{-3}\sqrt{(4+t-18t^2-31t^3)/t} - 36 - 116t\right]\right)^{1/3} \\ &- \frac{(1-\sqrt{-3})(3+t)}{3t^2}\left(t^2\left[12\sqrt{-3}\sqrt{(4+t-18t^2-31t^3)/t} - 36 - 116t\right]\right)^{-1/3}. \end{aligned} \tag{18}$$

The radius of convergence t_2 of g_2 can be determined by locating the branch points in the above; these are due to the square root and cube root factors above, and one may show that

$$t_2 = \frac{(43\,551 + 4836\sqrt{78})^{1/3}}{93} + \frac{139}{31(43\,551 + 4836\sqrt{78})^{1/3}} - \frac{6}{31} \approx 0.383\,0363\ldots. \tag{19}$$

The radius of convergence of g_2 may be determined without solving explicitly for it. In particular, the real solutions of equation (17) are given by the intersections of the curves $Y = g - 1$ and $Y = t^2 g^2 + t^3 g^3$ in the gY-plane, for any fixed value of t. I illustrate this in figure 7.

In figure 7, the value of the critical point t_2 is determined by examining intersections of $Y = g - 1$ and the curve $Y = t^2 g^2 + t^3 g^3$, which is convex for positive g. There are at most two non-negative real solutions g_+ and g_-. Increasing t moves these solutions closer to one another, and at a critical value t_2 there is only one solution $g_2^* = g_2(t_2) = g_+ = g_-$. For larger t, the solutions branch off into complex space and there are no real positive solutions. Thus, t_2 is the radius of convergence of g_2 and $g_2(t_2) = g^*$ is the value of the generating function at its critical value.

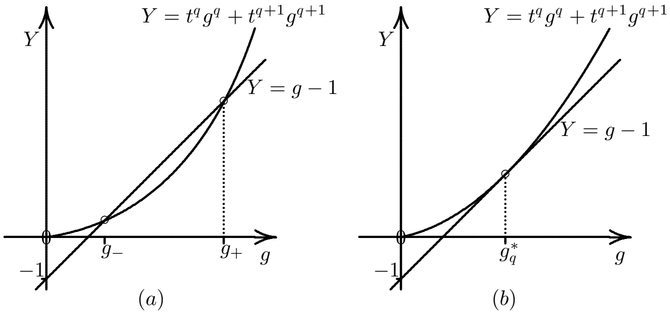

Figure 7. The radius of convergence t_2 of $g_2(t)$ can be determined by arguing as in this figure. Put $q = 2$ and observe that real solutions of $t^3 g_2^3 + t^2 g_2^2 - g_2 + 1 = 0$ may be determined by considering the intersections of the line $Y = g - 1$ with the curve $Y = t^2 g^2 + t^3 g^3$ in the gY-plane. If $t < t_2$ then the situation is as in (a): there are two real and non-negative solutions and $g_2(t)$ is given by the smaller real root (indicated by g_-). Increasing t to a value larger than t_2 will remove the intersections between the two curves and there are then no non-negative real values of g where the curves intersect. At the critical point $t = t_2$ the situation is illustrated in (b). There is one real solution for non-negative t at $g = g_2^* = g_2(t_2)$. As $t \nearrow t_2^-$, the two roots $g_2^{\pm}$ in (a) coalesce at $g = g_2^*$ and then they branch off into complex space for $t > t_2$.

To determine t_2 and g^*, observe that when $t = t_2$, then the line $Y = g - 1$ is tangent to the curve $Y = t^2 g^2 + t^3 g^3$, and moreover it passes through the point (t_2, g^*). The tangent is

$$Y = \left(2t_2^2 g^* + 3t_2^3 (g^*)^2\right) g - t_2^2 (g^*)^2 - 2t_2^3 (g^*)^3, \tag{20}$$

and this is the same as $Y = g - 1$ when $t = t_2$ critical point. In other words, by comparing the coefficient of g and the constant term, it follows that t_2 and g^* are the solutions of

$$2t_2^2 g^* + 3t_2^3 (g^*)^2 = 1 \qquad t_2^2 (g^*)^2 + 2t_2^3 (g^*)^3 = 1. \tag{21}$$

Solving these gives

$$t_2 = \frac{(43\,551 + 4836\sqrt{78})^{1/3}}{93} + \frac{139}{31(43\,551 + 4836\sqrt{78})^{1/3}} - \frac{6}{31},$$

$$g_2(t_2) = g^* = \frac{37}{24} + \left(\frac{49}{3336} - \frac{5\sqrt{78}}{2502}\right)(43\,551 + 4836\sqrt{78})^{1/3} + \left(\frac{913}{1391\,112} - \frac{16\sqrt{78}}{173\,889}\right)(43\,551 + 4836\sqrt{78})^{2/3}. \tag{22}$$

Evaluating t_2 and $g_2(t_2)$ gives $t_2 = 0.383\,0363\ldots$ and $g_2(t_2) = 1.716\,0204\ldots$. By eliminating t_2 in the pair of equations (21), one may show that $g^* = g_2(t_2)$ satisfies the polynomial

$$8[g^*]^3 - 37[g^*]^2 + 58[g^*] - 31 = 0, \tag{23}$$

with real root given by equation (22).

3.2. *q-Motzkin paths*

The above results can be generalized to q-Motzkin paths in a q-wedge. The generating function g_q satisfies the polynomial in equation (16). Generally, the roots of this polynomial cannot be determined explicitly. However, the radius of convergence t_q and the value of $g_q(t)$ at $t = t_q$ may be determined by using the arguments in figure 7. By determining the tangent to the curve $Y = t^{q+1}g^{q+1} + t^q g^q$ at $t = t_q$ and comparing it to the line $Y = g - 1$, the result is that one can solve for the critical point t_q and for $g^* = g_q(t_q)$ simultaneously from the set of equations

$$t_q^q (g^*)^{q-1}((q+1)t_q g^* + q) = 1 \qquad t_q^q (g^*)^q (q t_q g^* + (q-1)) = 1. \tag{24}$$

Eliminating t_q in this set of equations shows that $g^* = g_q(t_q)$ satisfies the polynomial

$$((q-1)g^* - q)^q + (1 + q(1 - g^*))^{q+1} = 0, \tag{25}$$

and this reproduces equation (23) when $q = 2$.

It is possible to determine an asymptotic expression in q for $g_q(t_q)$ from equation (25). Suppose that

$$g^* = g_q(t_q) = 1 + U/q \tag{26}$$

and substitute this into equation (25). After simplification one obtains

$$U = \frac{q}{q-1}(1 + (1-U)(1-U)^{1/q}). \tag{27}$$

Assume next that q is large and that $(1-U)^{1/q} \approx (1 - U/q)$. Substituting this into the above and solving for U in the resulting quadratic shows that

$$U \approx q(1 - \sqrt{1 - 2/q}) = 1 + 1/2q + O(1/q^2). \tag{28}$$

In other words, $U \to 1^+$ as $q \to \infty$, and the assumption that $g^* = 1 + U/q$ above is valid. This shows that

$$g^* = g_q(t_q) \approx 2 - \sqrt{1 - 2/q}. \tag{29}$$

This expression is quite accurate for larger values of q. For example, numerical solutions of equations (24) give $g_5(t_5) = 1.227\,193\,408\ldots$, $g_{10}(t_{10}) = 1.106\,041\,244\ldots$ and $g_{100}(t_{100}) = 1.010\,051\,581\ldots$, while this approximation shows that $g_5(t_5) \approx 1.225\,403\,331\ldots$, $g_{10}(t_{10}) \approx 1.105\,572\,809\ldots$ and $g_{100}(t_{100}) \approx 1.010\,050\,506\ldots$.

4. *r*-Motzkin paths

Fix q/p a non-negative rational number, and let (p, q) be a pair of relative prime and non-negative integers. Assume that $q \geqslant p$ and fix N, a (large) positive integer.

Let $p_x \in [0, 1]$ and $p_y \in [0, 1]$ be fixed such that $0 \leqslant p_x + p_y \leqslant 1$. Consider NE-oriented paths of length N with $\lfloor p_x N \rfloor$ horizontal edges and $\lfloor p_y N \rfloor$ vertical edges. These paths will have $N - \lfloor p_x N \rfloor - \lfloor p_y N \rfloor$ diagonal edges. The number of these paths of length N steps is given by the trinomial coefficient

$$c_N(p_x, p_y) = \binom{N}{\lfloor p_x N \rfloor, \lfloor p_y N \rfloor, N - \lfloor p_x N \rfloor - \lfloor p_y N \rfloor}. \tag{30}$$

If these paths start at the origin, then their final vertex has coordinates $(N - \lfloor p_y N \rfloor, N - \lfloor p_x N \rfloor)$. In other words, these NE-oriented paths are completely contained in the rectangle defined by opposing vertices at $(0, 0)$ and $(N - \lfloor p_y N \rfloor, N - \lfloor p_x N \rfloor)$.

Lemma 4.1. *Let $p_x \in [0, 1]$ and $p_y \in [0, 1]$ be fixed such that $0 \leqslant p_x + p_y \leqslant 1$. The limit as $N \to \infty$ of $c_N^{1/N}(p_x, p_y)$ is given by*

$$\lim_{N\to\infty} [c_N(p_x, p_y)]^{1/N} = \frac{1}{p_x^{p_x} p_y^{p_y} (1 - p_x - p_y)^{1-p_x-p_y}}.$$

The right-hand side has a maximum at $p_x = p_y = 1/3$. In that case, the value of the limit is 3.

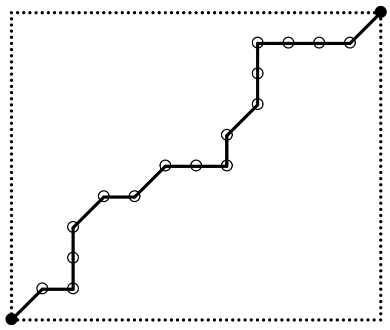

Figure 8. An NE-oriented lattice path crossing a rectangle from its bottom left-hand corner to its top right-hand corner.

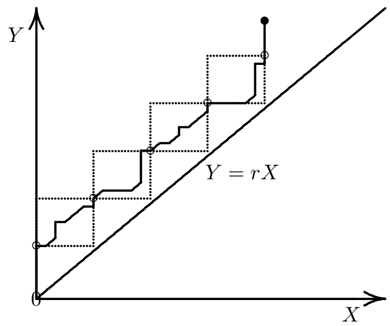

Figure 9. An NE-oriented path above the line $Y = rX$ can be constructed by joining NE-oriented paths crossing a sequence of rectangles of dimensions $\lfloor p_N \rfloor \times \lfloor q_N \rfloor$ at opposite vertices, and then joining the origin to the first vertex. Extend the path by adding s north edges after its final vertex. This gives an NE-oriented path of length $NM + s + q_N$ in the r-wedge formed by the Y-axis and the line $Y = rX$.

Proof. This can be computed directly by using Stirling's approximation for the factorials in the trinomial coefficient in equation (30). □

Let $R(a, b)$ be a rectangle of dimensions $p \times q$ with bottom left-hand vertex at (a, b) in the square lattice. An NE-oriented lattice path *crosses* $R(a, b)$ if its first vertex is at (a, b) and its final vertex is at the top right-hand corner of $R(a, b)$ and has coordinates $(a + p, b + q)$. In figure 8, an NE-oriented path crossing a rectangle of dimensions 10×12 is illustrated. The paths counted by $c_N(p_x, p_y)$ in equation (30) cross a rectangle $R(0, 0)$ of dimensions $(N - \lfloor Np_y \rfloor) \times (N - \lfloor Np_x \rfloor)$.

Let $r \geqslant 1$ be a real number. Let $\langle q_N/p_N \rangle$ be a sequence of rational numbers such that $[q_N/p_N] \to r$ as $N \to \infty$ and such that $[q_N/p_N] > r$ for each $N \geqslant 1$. If $\frac{1-p_x}{1-p_y} = r$, where $0 \leqslant p_x + p_y \leqslant 1$, then it would be suitable to define $q_N = N - \lfloor Np_x \rfloor$ and $p_N = N - \lceil Np_y \rceil$. Observe that $c_N(r) \geqslant c_N(q_N/p_N)$, since I assumed that $[q_N/p_N] > r$ for each $N \geqslant 1$.

Let n be a large positive integer and define M by $n = NM + s$, where $s \in [0, N)$. Stack the M rectangles $R((m - 1)p_N, mq_N)$ for $m = 1, 2, 3, \ldots, m$ of dimensions $p_N \times q_N$ by placing the bottom left-hand corner of $R(mp_N, (m + 1)q_N)$ on top of the top right-hand corner of $R((m - 1)p_N, mq_N)$, as illustrated in figure 9. Consider paths of length N with $\lfloor Np_x \rfloor$ horizontal edges and with $\lfloor Np_y \rfloor$ vertical edges crossing each rectangle. The path obtained by concatenating the paths crossing each rectangle $R((m-1)p_N, mq_N)$ has length NM and starts from the vertex $(0, q_N)$ and terminates in the vertex $((M-1)p_N, Mq_N)$. Append a set of q_N vertically oriented edges to join the path to the origin and a set of s vertical edges at its last edge. Then the total length of the path is $NM + s + q_N = n + q_N$. Since the rectangles are all disjoint with the line $Y = rX$, all paths constructed in this way are also counted by $c_{n+q_N}(r)$. In other words, if $n = NM + s$, then

$$c_{n+q_N}(r) \geqslant [C_N(p_x, p_y)]^M, \tag{31}$$

for any pair (p_x, p_y) such that $0 \leqslant p_x + p_y \leqslant 1$ and $\frac{1-p_x}{1-p_y} = r$. These arguments are enough to prove the following lemma.

Lemma 4.2. *Let r be a real number and suppose that (p_x, p_y) is a point in the unit square $[0,1]^2$ where $0 \leqslant p_x + p_y \leqslant 1$, such that $\frac{1-p_x}{1-p_y} = r$. Then,*

$$\lim_{n\to\infty} [c_n(r)]^{1/n} \geqslant [C_N(p_x, p_y)]^{1/N}$$

for any $N \geqslant 1$.

Proof. Observe that $c_n(r)$ is an increasing function of n. Thus, if $n = NM + s$, then the limit

$$\lim_{n\to\infty} [c_n(r)]^{1/n} = \lim_{M\to\infty} [c_{NM+s+q_N}(r)]^{1/(NM+s)}$$

exists. By the inequality in equation (31), one sees that

$$\left[c_{NM+s+q_N}(r)\right]^{1/(NM+s)} \geqslant [C_N(p_x, p_y)]^{M/(NM+s)}.$$

Fix N and let $M \to \infty$. This proves the lemma. □

By taking $N \to \infty$ in lemma 4.2, the immediate corollary to lemmas 4.1 and 4.2 is

Corollary 4.3. *Let $r > 0$ be a real number and let p_x and p_y be real numbers in the unit square such that $0 \leqslant p_x + p_y \leqslant 1$ and $(1 - p_x) = r(1 - p_y)$. Then,*

$$\lim_{n\to\infty} [c_n(r)]^{1/n} \geqslant \sup_{p_x, p_y} \left[\frac{1}{p_x^{p_x} p_y^{p_y} (1 - p_x - p_y)^{1-p_x-p_y}}\right]$$

where the supremum is taken subject to $0 \leqslant p_x + p_y \leqslant 1$ and $(1 - p_x) = r(1 - p_y)$.

One may also bound $c_n(r)$ from above by NE-oriented paths of length n with endpoint confined in the r-wedge formed by the Y-axis and the line $Y = rX$. One such path is illustrated in figure 10. Consider paths of length n, with N horizontal and M vertical edges and with $n - N - M$ edges oriented in the diagonal direction. The endpoint of this path has coordinates $(n - M, n - N)$, and so M and N are constrained by $(n - N) \geqslant r(n - M)$. In addition $N + M \leqslant n$. Thus,

$$c_n(r) \leqslant \sum_{N,M\geqslant 0} \binom{n}{N, M, n-N-M} \tag{32}$$

where the summation is constrained by $N + M \leqslant n$ and $(n - N) \geqslant r(n - M)$. The number of possible endpoints is at most n^2, and one may choose N and M to maximize the right-hand side above. Introduce (p_x, p_y) such that $\lfloor np_x \rfloor = N$ and $\lfloor np_y \rfloor = M$. The bound on $c_n(r)$ may be written as

$$c_n(r) \leqslant n^2 \sup_{0\leqslant p_x, p_y\leqslant 1} \binom{n}{\lfloor np_x\rfloor, \lfloor np_y\rfloor, n - \lfloor np_x\rfloor - \lfloor np_y\rfloor}, \tag{33}$$

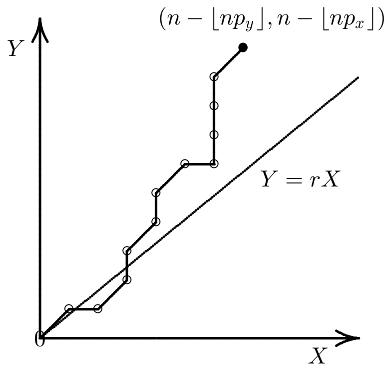

Figure 10. An NE-oriented path with endpoint above the line $Y = rX$. The endpoint can be selected at any vertex in a region of area smaller than n^2. If this path has $\lfloor np_x \rfloor$ east edges and $\lfloor np_y \rfloor$ north edges, then it has $\ell = (n - \lfloor np_x \rfloor - \lfloor np_y \rfloor)$ edges in the north-east direction and it ends in the vertex with coordinates $(\ell + \lfloor np_x \rfloor, \ell + \lfloor np_y \rfloor) = (n - \lfloor np_y \rfloor, n - \lfloor np_x \rfloor)$. In other words, p_x and p_y are such that $n - \lfloor np_x \rfloor \geqslant r(n - \lfloor np_y \rfloor)$. Also observe that $\leqslant p_x + p_y \leqslant 1$.

where the supremum is taken subject to the constraints that $n \geqslant \lfloor np_x \rfloor + \lfloor np_y \rfloor$ and $n - \lfloor np_x \rfloor \geqslant r(n - \lfloor np_y \rfloor)$. The inequality in equation (33) is enough to prove the following lemma:

Lemma 4.4. *Let $r > 0$ be a real number and let p_x and p_y be real numbers in the unit square such that $0 \leqslant p_x + p_y \leqslant 1$ and $(1 - p_x) \geqslant r(1 - p_y)$. Then,*

$$\lim_{n\to\infty} [c_n(r)]^{1/n} \leqslant \sup_{p_x, p_y} \left[\frac{1}{p_x^{p_x} p_y^{p_y} (1 - p_x - p_y)^{1-p_x-p_y}} \right]$$

where the supremum is taken subject to $0 \leqslant p_x + p_y \leqslant 1$ and $1 - p_x \geqslant r(1 - p_y)$.

Proof. Take the $1/n$-power of the inequality in equation (33) and take n to infinity. The lemma follows directly. □

Let

$$g_r = \sum_{n=0}^{\infty} c_n(r) t^n \tag{34}$$

be the generating function of NE-oriented paths in the r-wedge formed by the Y-axis and the line $Y = rX$, where r is irrational. For any value of $r \in [0, \infty)$, observe that

$$c_n(r) \leqslant 3^n \tag{35}$$

and the radius of convergence of g_r is bounded by

$$t_r \geqslant \lim_{n\to\infty} \sup [c_n(r)]^{-n} = \tfrac{1}{3}. \tag{36}$$

This can also be seen from lemma 4.4; the supremum on the right hand side is realized when $p_x = p_y = 1/3$ if the constraints are ignored.

Also observe that t_r is monotonically increasing with increasing r. If $r = 1$, then the bounds in corollary 4.3 and lemma 4.4 coincide, and thus $t_1 = 1/3$ is the radius of convergence of $g_r(t)$. Equation (36) shows that as $r \to 0^+$, then $t_{0^+} \geqslant 1/3$, and since t_r is an increasing function for $r > 0$, the result is that

$$t_r = 1/3, \qquad \text{for irrational } r \in (0, 1). \tag{37}$$

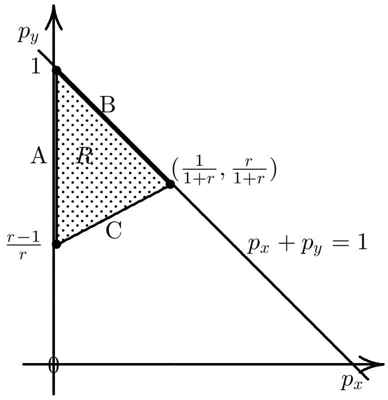

Figure 11. The region R enclosed by the line $(1 - p_x) = r(1 - p_y)$, the line $p_x = 0$ and $0 \leqslant p_y \leqslant 1$, and the line $p_x + p_y = 1$ in the (p_x, p_y)-plane. Since $\nabla f(p_x, p_y) \neq 0$ anywhere in R if $r > 1$, the maximum of $f(p_x, p_y)$ is on the boundary of R.

Since t_r is a non-increasing function, this result implies that $t_r = 1/3$ for all real $r \in [0, 1]$.

Suppose that $r > 1$ instead. In this instance one would be interested in the function

$$f(p_x, p_y) = \frac{1}{p_x^{p_x} p_y^{p_y} (1 - p_x - p_y)^{1-p_x-p_y}}. \tag{38}$$

This function has a global maximum at $p_x = p_y = 1/3$, when $f(1/3, 1/3) = 3$.

Consider now the line $Y = rX$. Above this line the function $f(p_x, p_y)$ is defined on the (triangular) region R (see figure 11) enclosed by the line $(1 - p_x) = r(1 - p_y)$, the line $p_x = 0$ and by $0 \leqslant p_y \leqslant 1$ and also by the line $p_x + p_y = 1$. $f(p_x, p_y)$ is differentiable in the interior of R and its gradient is not zero anywhere in the interior of R for any irrational $r > 1$. Thus, the local maximum of $f(p_x, p_y)$ on R is on the boundary of R.

R is a triangular region with three corners in the (p_x, p_y)-plane with coordinates $\left(0, \frac{r-1}{r}\right)$, $(0, 1)$ and $\left(\frac{1}{1+r}, \frac{r}{1+r}\right)$. This region is illustrated in figure 11. On the part of the boundary marked by A in figure 11 the maximum of $f(p_x, p_y)$ is $f(0, 1/2) = 2$ if $r \in [1, 2]$ and $f(0, (r-1)/r) = r/(r-1)^{(r-1)/r}$ if $r > 2$. In other words,

$$\sup_A f(p_x, p_y) = \begin{cases} 2, & \text{if} \quad r \in [1, 2], \\ \dfrac{r}{(r-1)^{(r-1)/r}}, & \text{if} \quad r > 2. \end{cases} \tag{39}$$

On the part of the boundary marked by B in figure 11, note that $p_x = 1 - p_y$ and $p_x \in [0, 1/(1+r)]$. If $r \leqslant 1$, then the maximum of $f(p_x, p_y)$ along B is $f(1/2, 1/2) = 2$; otherwise, for $r > 1$, the maximum is $f(1/(1+r), r/(1+r)) = (1+r)/r^{r/(1+r)}$. In other words,

$$\sup_B f(p_x, p_y) = \begin{cases} 2, & \text{if} \quad r \in [0, 1], \\ \dfrac{1+r}{r^{r/(1+r)}}, & \text{if} \quad r > 1. \end{cases} \tag{40}$$

Along the boundary marked by C the supremum is more difficult to compute. In this case, $1 - p_x = r(1 - p_y)$ and $p_x \in [0, 1/(1+r)]$. Eliminating p_x shows that

$$\sup_C f(p_x, p_y) = \sup_{p_y \in [(r-1)/r, r/(1+r)]} \left\{ \frac{1}{p_y^{p_y} (1 - r(1-p_y))^{1-r(1-p_y)} (r(1-p_y) - p_y)^{r(1-p_y)-p_y}} \right\}. \tag{41}$$

Suppose that $p_x = 1/(2r+1)$. Then, $p_y = (2r-1)/(2r+1)$ and one observes that (p_x, p_y) is on the line segment C, while $(r-1)/r \leqslant (2r-1)/(2r+1) \leqslant r/(r+1)$ for $r > 1$. Evaluating $f(p_x, p_y)$ at this point shows that

$$\sup_C f(p_x, p_y) \geqslant \frac{2r+1}{(2r-1)^{(2r-1)/(2r+1)}}. \tag{42}$$

Finally, note that

$$\begin{aligned} \sup_C f(p_x, p_y) &\geqslant \frac{2r+1}{(2r-1)^{(2r-1)/(2r+1)}} \geqslant \frac{r}{(r-1)^{(r-1)/r}} = \sup_A f(p_x, p_y) \\ \sup_C f(p_x, p_y) &\geqslant \frac{2r+1}{(2r-1)^{(2r-1)/(2r+1)}} \geqslant \frac{1+r}{r^{r/(1+r)}} = \sup_B f(p_x, p_y), \end{aligned} \tag{43}$$

where the first inequality is valid for $r \geqslant 2$ and the second for any $r \geqslant 1$. Since the lower bound in equation (42) is bigger or equal to 2 for any $r \in [1, 2]$, the inequality $\sup_C f(p_x, p_y) \geqslant \sup_A f(p_x, p_y)$ is also valid if $r \in [1, 2]$. Thus, the supremum of $f(p_x, p_y)$ over the region R is achieved in a point on the line segment marked by C in figure 11 for any $r \geqslant 1$.

Since the line-segment C in figure 11 is given by the formula $1 - p_x = r(1 - p_y)$ for $r \geqslant 1$, the supremum in lemma 4.4 is determined by a point on this line. In other words, one may replace the restriction $1 - p_x \geqslant r(1 - p_y)$ in lemma 4.4 by the stronger restriction $1 - p_x = r(1 - p_y)$. Comparison with corollary 4.3 gives the following theorem.

Theorem 4.5. *Let $r > 0$ be a real number and let p_x and p_y be real numbers in the unit square such that $0 \leqslant p_x + p_y \leqslant 1$ and $(1 - p_x) = r(1 - p_y)$. Then,*

$$\lim_{n\to\infty} [c_n(r)]^{1/n} = \sup_{p_x, p_y} \left[\frac{1}{p_x^{p_x} p_y^{p_y} (1 - p_x - p_y)^{1-p_x-p_y}} \right]$$

where the supremum is taken subject to $0 \leqslant p_x + p_y \leqslant 1$ and $(1 - p_x) = r(1 - p_y)$.

This theorem completes the characterization of the radius of convergence of the generating function g_r in equation (34). I showed that for $0 \leqslant r \leqslant 1$ the radius of convergence is given by $t_r = 1/3$ in equation (36). By theorem 4.5 the corollary is the following.

Corollary 4.6. *The radius of convergence of $g_r(t) = \sum_{n\geqslant 0} c_n(r) t^n$ is given by*

$$t_r = \begin{cases} \frac{1}{3}, & \text{if} \quad r \in [0, 1], \\ \left[\sup_{p_x, p_y} \left[\frac{1}{p_x^{p_x} p_y^{p_y} (1 - p_x - p_y)^{1-p_x-p_y}} \right] \right]^{-1}, & \text{if} \quad r > 1, \end{cases}$$

where the supremum is taken subject to the constraints that $0 \leqslant p_x + p_y \leqslant 1$ and $1 - p_x = r(1 - p_y)$.

This completes the proofs of the claims made in the abstract and in equation (8).

5. Forces in Motzkin paths in an *r*-wedge

The expressions in corollary 4.6 can be used to determine the forces exerted by an NE-oriented path on the boundaries of an r-wedge. The situation is illustrated in figure 5(*b*). The generating function g_r of the NE-oriented paths has radius of convergence t_r as in corollary 4.6, and the limiting free energy in this model is given by $\mathcal{F}(r) = -\log t_r$. The entropic forces in this model are given by the derivative of $\mathcal{F}(r)$, and an immediate consequence is that the net force on the r-wedge is zero for all $r \in [0, 1]$.

To determine forces for $r > 1$ requires the calculation of the limiting free energy. Thus, the supremum in corollary 4.6 must be determined. Some progress can be made by eliminating p_x using the relation $1 - p_x = r(1 - p_y)$. By writing the supremum as an infimum, the following is obtained:

Lemma 5.1. *Let $r > 1$, the radius of convergence of $g_r(t)$ is given by the infimum*

$$t_r = \min_{\frac{r-1}{r} \leqslant y \leqslant \frac{r}{r+1}} [y^y(1 - r(1 - y))^{1-r(1-y)}(r(1 - y) - y)^{r(1-y)-y}].$$

Furthermore, if y_0 is the positive root of

$$(r(1 - y) - y)^{r+1} - y(1 - r(1 - y))^r = 0$$

in the interval $\left[\frac{r-1}{r}, \frac{r}{r+1}\right]$, then t_r is given by

$$t_r = y_0^{y_0}(1 - r(1 - y_0))^{1-r(1-y_0)}(r(1 - y_0) - y_0)^{r(1-y_0)-y_0}$$

where y_0 is a function of r.

Proof. Let $f(p_x, p_y)$ be as in equation (38), and substitute $p_x = 1 - r(1 - p_y)$. Put $y = p_y$ to simplify the notation. Then, the constraint $0 \leqslant p_x + p_y \leqslant 1$ in corollary 4.6 becomes $\frac{r-1}{r} \leqslant y \leqslant \frac{r}{r+1}$. Next observe that $\left[\frac{r-1}{r}, \frac{r}{r+1}\right]$ is a compact interval, so one may replace the supremum in corollary 4.6 by a maximum. Change the maximum into a minimum by noting that $\max_x[1/f(x)] = [\min_x f(x)]^{-1}$ on a compact interval. This proves the first part of the lemma.

Next, define

$$h(y) = \frac{1}{y^y(1 - r(1 - y))^{1-r(1-y)}(r(1 - y) - y)^{r(1-y)-y}}$$

so that $t_r = \left[\max_{\frac{r-1}{r} \leqslant y \leqslant \frac{r}{r+1}}[h(y)]\right]^{-1}$. Observe that

$$\frac{\mathrm{d}h(y)}{\mathrm{d}y} = \frac{(1 + r)\log(r(1 - y) - y) - r\log(1 - r(1 - y)) - \log y}{y^y(1 - r(1 - y))^{1-r(1-y)}(r(1 - y) - y)^{r(1-y)-y}}.$$

This derivative is zero if

$$(1 + r)\log(r(1 - y) - y) - r\log(1 - r(1 - y)) - \log y = 0$$

or equivalently, if

$$(r(1 - y) - y)^{r+1} - y(1 - r(1 - y))^r = 0.$$

Let $y_0 > 0$ be a root of this function in the interval $[(r - 1)/r, r/(1 + r)]$. That y_0 exists follows from the observation that if $y = (r - 1)/r$, then

$$(r(1 - y) - y)^{r+1} - y(1 - r(1 - y))^r = \frac{1}{r^{r+1}} > 0$$

and if $y = r/(1 + r)$, then

$$(r(1 - y) - y)^{r+1} - y(1 - r(1 - y))^r = \frac{-r}{(1 + r)^{1+r}} < 0.$$

Since $(r(1 - y) - y)^{r+1} - y(1 - r(1 - y))^r$ is a continuous real function on $[(r - 1)/r, r/(1 + r)]$ for any fixed $r > 1$, it follows by Rolle's theorem that it has a root in this interval. Also observe that $(r(1 - y) - y)^{r+1}$ is a strictly decreasing function of y on $[(r - 1)/r, r/(1 + r)]$ and $y(1 - r(1 - y))^r$ is a strictly increasing function of y on $[(r - 1)/r, r/(1 + r)]$. Thus,

Table 1. Numerical and asymptotic estimates of y_0.

r	y_0 numerical	y_0 by equation (46)
2	0.5827 ...	0.6033 ...
5	0.8148 ...	0.8168 ...
10	0.904 13 ...	0.904 42 ...
20	0.951 113 ...	0.951 156 ...
40	0.975 2922 ...	0.975 2980 ...
80	0.987 575 21 ...	0.987 575 98 ...
160	0.993 769 12 ...	0.993 769 22 ...

there is only one solution y_0 in $[(r-1)/r, r/(1+r)]$ of $(r(1-y)-y)^{r+1} = y(1-r(1-y))^r$. This solution determines the infimum and thus the value of t_r. This completes the proof. □

The radius of convergence t_r of g_r could be determined if the root y_0 is known. Generally, there appears to be no closed-form solution y_0 of $(r(1-y)-y)^{1+1/r} - y^{1/r}(1-r(1-y)) = 0$, and so other methods should be explored. In the next sections, I will estimate y_0 first asymptotically (for large values of r) and then compare the results to numerical solutions.

5.1. Asymptotic determination of y_0

Guess the solution $y_0 = (r-1)/r + B/r^2 + C\log(r)/r^3 + \cdots$ and substitute for y into

$$(r(1-y)-y)^{1+1/r} - y^{1/r}(1-r(1-y)) = 0. \tag{44}$$

Expand the terms in this equality asymptotically and collect the terms with the same dependence on r. This in particular shows that

$$\frac{1-2B}{r} + \frac{(B-1-2C)\log(r)}{r^2} + O\left(\frac{1}{r^2}\right) = 0. \tag{45}$$

In other words, $1-2B = 0$ and $B-1-2C = 0$. Solving for B and C shows that the appropriate asymptotic expression for y_0 is

$$y_0 = \frac{r-1}{r} + \frac{1}{2r^2} - \frac{\log(r)}{4r^3} + O\left(\frac{1}{r^3}\right). \tag{46}$$

This expression for y_0 is remarkably accurate. In table 1 estimates for y_0 from equation (46) are compared to numerical values for y_0; with increasing r the asymptotic formula quickly becomes accurate to many significant digits.

Substitution of the asymptotic formula for y_0 into lemma 5.1 gives an estimate for t_r, and thus for the free energy in this model, defined by

$$\mathcal{F}(r) = -\log t_r. \tag{47}$$

Substituting for t_r and expanding again shows that

$$\mathcal{F}(r) \simeq \frac{1+\log(2r)}{r} - \frac{1+\log(2r)}{r^2} + \frac{2+6\log(r)+3\log^2(r)+6\log 2\log(r)}{24r^3}, \tag{48}$$

in the regime where $r \to \infty$. One may take the derivative of this to r to estimate the magnitude of the force as $r \to \infty$ (that is, in the regime that the wedge becomes very narrow). This gives

$$F(r) = \frac{\log(2r)}{r^2} - \frac{1+2\log(2r)}{2r^3} + O\left(\frac{\log(2r)}{r^4}\right), \tag{49}$$

as $r \to \infty$. In other words, the force approaches zero with leading term $\log(2r)/r^2$. A similar observation was made in a model of fully directed paths in the square lattice. In that case, the force approaches zero proportional to $\log(r)/r^2$ as $r \to \infty$ [15].

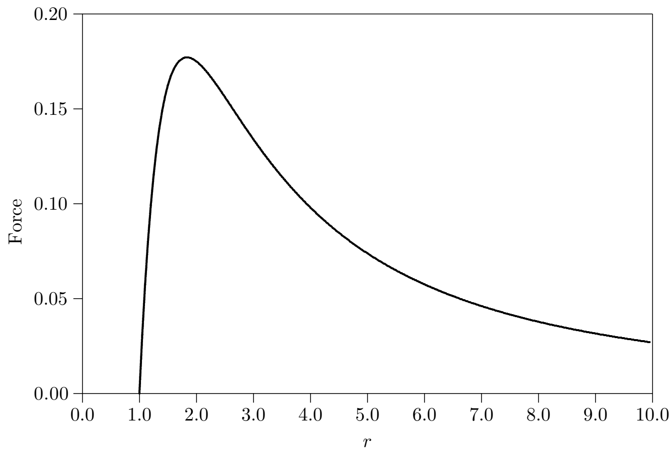

Figure 12. The magnitude of the force of an NE-oriented path in an r-wedge formed by the Y-axis and the line $Y = rX$ as a function of r. The force goes through a maximum at $r = 1.833\,60\ldots$ where its magnitude is $0.177\,169\ldots$.

Table 2. Numerical and asymptotic estimates of $F(r)$.

r	$F(r)$ numerical	$F(r)$ by equation (49)
2	$0.175\ldots$	$0.111\ldots$
5	$0.0738\ldots$	$0.0697\ldots$
10	$0.026\,91\ldots$	$0.026\,46\ldots$
20	$0.008\,741\ldots$	$0.008\,699\ldots$
40	$0.002\,6661\ldots$	$0.002\,6625\ldots$
80	$0.000\,782\,41\ldots$	$0.000\,782\,11\ldots$
160	$0.000\,223\,82\ldots$	$0.000\,223\,79\ldots$

5.2. Numerical determination of the force

The free energy can be determined numerically as a function of r by solving for the root in lemma 5.1. By taking numerical derivatives of the free energy with respect to r, one determines numerical estimates of the magnitude of the force that the path exerts on the boundaries of the r-wedge. This was done for $r \in [1, 10]$ in figure 12; for $r \in [0, 1]$, I have already noted that the net force is zero.

The general shape of the curve in figure 12 is similar to the results obtained for fully directed paths in an r-wedge [15]. The force goes through a maximum at $r = 1.833\,60\ldots$; this occurs at a wedge with vertex angle $\alpha = 1.071\,51\ldots$. This is close to the number $(1 + \pi)/2 = 1.070\,79\ldots$, but I could not determine if this coincidence is meaningful. The force in the model of fully directed paths in [15] achieved its maximum at a vertex angle close to $\pi/7$, in contrast to the result here.

The asymptotic formula for the force $F(r)$ in equation (49) can be compared to the numerical values obtained for $F(r)$. Comparisons are listed in table 2. The accuracy increases with increasing r.

The force may similarly be computed as a function of the vertex angle α instead. This changes the force into a moment about the origin. This moment is plotted in figure 13 as a function of α. The moment diverges as $\alpha \to 0^+$ and decays to zero as $\alpha \nearrow \pi/4$, as expected by considering corollary 4.6.

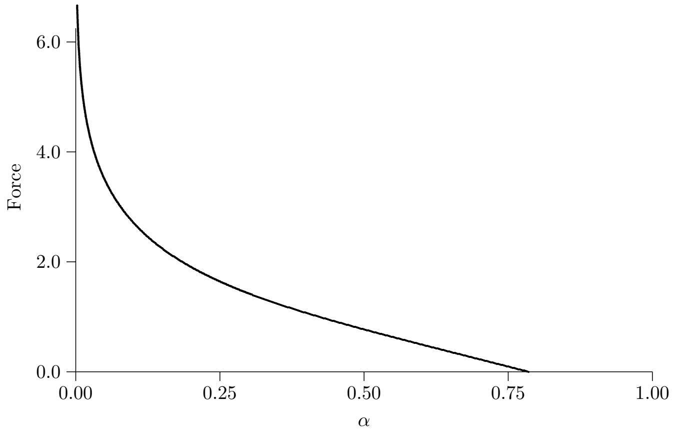

Figure 13. The moment of the force of an NE-oriented path in an r-wedge about the origin as a function of the vertex angle α.

The divergence of the moment of the force as the vertex angle α tends to zero is logarithmic. This may be demonstrated by changing variables to α in equation (49):

$$F(\alpha) = \log(2/\alpha) - (\alpha/2)(1 + 2\log(2/\alpha) + O(\alpha^2 \log(2/\alpha)) \qquad \text{as} \quad \alpha \to 0^+. \tag{50}$$

Numerical integration of the force shows that the total amount of work done to close the r-wedge from any vertex angle larger than $\pi/4$ to zero is $1.085\,07\ldots$ units.

6. An alternative ensemble of Motzkin paths

In section 4, models of r-Motzkin paths confined in r-wedges were examined. In these models, the edge-generating variable was t, irrespective of the type of edge. Unit length N- and E-edges were weighted by t each, as were NE-edges of length $\sqrt{2}$. In this section, an alternative model of r-Motzkin paths in r-wedges are considered, but with t generating another aspect of the paths.

Let $\mathcal{M}$ be an NE-oriented path from the origin above the line $Y = rX$, where $r > 0$ is an irrational number and with final vertex (a, b). The *span* of $\mathcal{M}$ is $a + b$. The number of NE-oriented paths above the line $Y = rX$ with span n is defined to be $m_r(n)$ and the generating function of these paths is

$$h_r = \sum_{n=0}^{\infty} m_r(n) t^n. \tag{51}$$

Observe that the span of a path with p E-edges, q N-edges and ℓ NE-edges is $p + q + 2\ell$, so that NE-edges are weighted by t^2 in the generating function h_r. This is in contrast with the models in the previous sections. As before, the radius of convergence t_r of h_r is required. This will be done by first considering paths crossing rectangles.

6.1. Paths crossing a rectangle

Consider NE-oriented paths from the origin to the point (p, q) of length at most $p + q$ and span equal to $p + q$. These paths cross the rectangle with opposite corners $(0, 0)$ and (p, q),

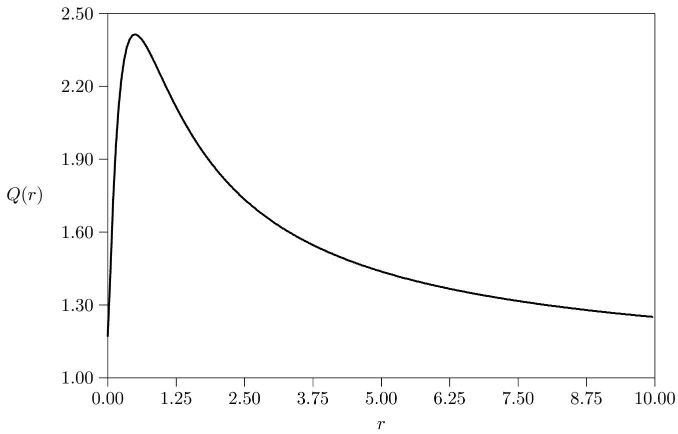

Figure 14. The function $Q(r)$ (see lemma 6.1) plotted against r. Observe that $Q(r) = Q(1/r)$ and that $Q(1)$ is the maximum of this function.

and by equation (14) the number of such paths is

$$Q(p,q) = \sum_{\ell=0}^{\min\{p,q\}} \binom{p+q-\ell}{p-\ell,\, q-\ell,\, \ell}, \tag{52}$$

since a path with ℓ NE-edges will have length $p+q-\ell$. The trinomial coefficients above are maximized if

$$\ell = \ell^* = \left\lfloor \frac{p+q-\sqrt{p^2+q^2}}{2} \right\rfloor + \epsilon \tag{53}$$

where $\epsilon = 0, 1$ is a small integer correcting for the effects of parity when the floor function is applied. Observe that $0 \leqslant \ell^* \leqslant \min\{p,q\}$. Thus, the number of paths crossing a $p \times q$-square is bounded by

$$\binom{p+q-\ell^*}{p-\ell^*,\, q-\ell^*,\, \ell^*} \leqslant Q(p,q) \leqslant [\min\{p,q\}] \binom{p+q-\ell^*}{p-\ell^*,\, q-\ell^*,\, \ell^*}. \tag{54}$$

Let $\langle q_n/p_n \rangle$ be a sequence of rational numbers with (p_n, q_n) a pair of relative prime and positive integers. Suppose, moreover, that $[q_n/p_n] \to r$, where $r > 0$ is an irrational number. As $n \to \infty$, both $q_n \to \infty$ and $p_n \to \infty$. The following lemma follows directly from equation (54).

Lemma 6.1. *Let $\langle q_n/p_n \rangle$ be a sequence of rational numbers with (p_n, q_n) a pair of relative prime and positive integers. Suppose, moreover, that $[q_n/p_n] \to r$, where $r > 0$ is an irrational number. Then,*

$$\lim_{n\to\infty} [Q(p_n, q_n)]^{1/(p_n+q_n)} = \frac{R_+(r)}{R_1(r) R_2(r) R_-(r)} = Q(r),$$

where

$$R_+(r) = ((1+r+\sqrt{1+r^2})/2)^{\frac{1+r+\sqrt{1+r^2}}{2(1+r)}} \qquad R_-(r) = ((1+r-\sqrt{1+r^2})/2)^{\frac{1+r-\sqrt{1+r^2}}{2(1+r)}}$$

$$R_1(r) = ((1-r+\sqrt{1+r^2})/2)^{\frac{1-r+\sqrt{1+r^2}}{2(1+r)}} \qquad R_2(r) = ((r-1+\sqrt{1+r^2})/2)^{\frac{r-1+\sqrt{1+r^2}}{2(1+r)}}.$$

Proof. Consider equation (54) with $(p, q) = (p_n, q_n)$. Take the power $1/(p_n + q_n)$, approximate the factorials in the trinomials by Stirling's approximation, and let $n \to \infty$. Since $[q_n/p_n] \to r$, the resulting limit is given by $Q(r)$ defined in terms of the functions $R_\pm(t)$ and $R_{1,2}(t)$. □

Observe that $Q(r) = Q(1/r)$, as one would expect (the number of NE-oriented paths ending in (p, q) is the same as the number of NE-oriented paths ending in (q, p)). Moreover, $\sup_{r>0} Q(r) = Q(1) = 1 + \sqrt{2}$, so that paths ending in the line $Y = X$ dominates the limit in lemma 6.1.

6.2. *r-Motzkin paths*

Denote the number of q/p-Motzkin paths ending in the vertex (p, q) by $m_{p,q}$, and note that these paths have span $p + q$.

As before, let $\langle q_n/p_n\rangle$ be a sequence of rational numbers with (p_n, q_n) a pair of relative prime and positive integers. Suppose, moreover, that $[q_n/p_n] \to r$, where $r > 0$ is an irrational number and that $[q_n/p_n] > r$ for each n. Then, it follows that

$$m_{p_n,q_n} \leqslant m_r(n) \qquad \text{where} \quad n = p_n + q_n. \tag{55}$$

On the other hand, paths counted by $m_r(n)$ can be bounded by paths of span n crossing a rectangle with right-most top-most vertex above the line $Y = rX$. Thus,

$$m_r(n) \leqslant (n+1)^2 \max_{q/p>r} [Q(p, q)] \qquad \text{where} \quad n = p + q. \tag{56}$$

Consider first an $r \in (0, 1)$. Choose $p_n = \lfloor n/2\rfloor$ and $q_n = \lceil n/2\rceil$ in equation (55). Then, $p_n + q_n = n$ and $[q_n/p_n] > r$, and by taking the power $1/n$ of equation (55) and then taking $n \to \infty$,

$$\liminf_{n\to\infty} [m_{\lfloor n/2\rfloor,\lceil n/2\rceil}]^{1/n} \leqslant \liminf_{n\to\infty} [m_r(n)]^{1/n}. \tag{57}$$

On the other hand, let $p = p_n$ and $q = q_n$ in equation (56) where $p_n + q_n = n$ for each n maximize the right-hand side. Then, by equation (56) it follows that

$$m_r(n) \leqslant (n+1)^2 [Q(p_n, q_n)]. \tag{58}$$

Take the power $1/n$ of this, and let $n \to \infty$ to determine the lim sup of the left-hand side. The lim sup of the right-hand side is less or equal to $\sup_{r\in(0,1)} Q(r)$, as in lemma 6.1. These arguments give the following lemma:

Lemma 6.2. *Suppose that* $r \in (0, 1)$. *Then,*

$$\liminf_{n\to\infty} [m_{\lfloor n/2\rfloor,\lceil n/2\rceil}]^{1/n} \leqslant \liminf_{n\to\infty} [m_r(n)]^{1/n} \leqslant \limsup_{n\to\infty} [m_r(n)]^{1/n} \leqslant \sup_{r\in(0,1)} Q(r) = Q(1).$$

Consider next the cases that $r > 1$. Inequality (56) gives the following lemma:

Lemma 6.3. *Suppose that* $r > 1$. *Then,*

$$\limsup_{n\to\infty} [m_r(n)]^{1/n} \leqslant Q(r)$$

where $Q(r)$ *is defined in lemma 6.1.*

Proof. Let $p_n + q_n = n$ be those values of p and q which maximizes the right hand side of equation (56). Then $[q_n/p_n] > r$,

$$m_r(n) \leqslant (n+1)^2 Q(p_n, q_n)$$

for each n. Take the power $1/n$ and let $n \to \infty$ to find the lim sup of the left-hand side. Since $[q_n/p_n] > r$ for each n, the result is that

$$\limsup_{n\to\infty}[m_r(n)]^{1/n} \leqslant \sup_{s\geqslant r} Q(s)$$

where lemma 6.1 was used. Observe that $Q(s)$ is a strictly decreasing function for $s > 1$, hence the supremum is found when $s = r$. This completes the proof. □

Similarly, the inequality (55) gives the following lemma:

Lemma 6.4. *Let $\langle q_n/p_n\rangle$ be a sequence of rational numbers with (p_n, q_n) a pair of relative prime and positive integers such that $p_n + q_n = n$ for each n. Suppose, moreover, that $[q_n/p_n] \to r$, where $r > 1$ is an irrational number. Then,*

$$\liminf_{n\to\infty}\left[m_{p_n,q_n}\right]^{1/n} \leqslant \liminf_{n\to\infty}[m_r(n)]^{1/n}. \tag{59}$$

Lemmas 6.2, 6.3 and 6.4 give certain bounds on the limits of $[m_r(n)]^{1/n}$. The next task is to prove existence of this limit and to compute its value at the same time. This is done next.

6.3. Calculating $\lim_{n\to\infty}[m_r(n)]^{1/n}$

In this section, I prove that $\lim_{n\to\infty}[m_r(n)]^{1/n} = Q(r)$ if $r > 1$ by showing that $\liminf_{n\to\infty}[M_r(n)]^{1/n} \geqslant Q(r)$. A by-product of the proof will be that $\liminf_{n\to\infty}[m_{\lfloor n/2\rfloor,\lceil n/2\rceil}]^{1/n} \geqslant Q(1)$, so that existence of $\lim_{n\to\infty}[m_r(n)]^{1/n}$ follows for all irrational $r > 0$ by lemma 6.2 and by lemmas 6.3 and 6.4.

Consider first $r > 1$. By lemma 6.4 existence of $\lim_{n\to\infty}[m_r(n)]^{1/n}$ would follow if one proves that $\liminf_{n\to\infty}\left[m_{p_n,q_n}\right]^{1/n} \geqslant Q(r)$. To show this, fix a large integer N, assume that $p_n + q_n = n$ and that $[q_n/p_n] \to r$ and $[q_n/p_n] > r$ as $n \to \infty$, where (p_n, q_n) are relative primes. Define the positive integers

$$a_n = \left\lfloor \frac{p_n}{N}\right\rfloor \qquad b_n = \left\lfloor \frac{q_n}{N}\right\rfloor \tag{60}$$

so that $p_n = Na_n + v_n$ and $q_n = Nb_n + u_n$ where $0 \leqslant v_n < a_n$ and $0 \leqslant u_n < b_n$.

Next, define the rectangle $R(a, b; c, d)$ to be that rectangle in the square lattice defined by its left-most bottom-most vertex (a, b) and by its right-most top-most vertex (c, d). Consider the sequence of M rectangles,

$$R((m-1)a_n, mb_n + 1; ma_n, (m+1)b_n + 1) \qquad \text{for} \quad m = 1, 2, \ldots, M, \tag{61}$$

of dimensions $a_n \times b_n$ and disjoint with the line $Y = (q_n/p_n)X$ and thus with $Y = rX$. This is illustrated in figure 15. M is determined by requiring both $(M + 1)b_n + 1 \leqslant q_n$ and $(M + 1)a_n + 1 \leqslant p_n$. That is, M is the largest integer such that $M \leqslant (p_n - 1)/a_n - 1$ and $M \leqslant (q_n - 1)/b_n - 1$. In other words, $M \geqslant \min\{(p_n - 1)/a_n - 2, (q_n - 1)/b_n - 2\}$ and so $\lim_{n\to\infty}[M/N] = 1$.

The number of paths crossing this sequence of rectangles is at least $[Q(a_n, b_n)]^M$, and moreover by construction these paths are disjoint with the line $Y = rX$. One may add edges from the origin to $(0, b_n)$ and from $(Ma_n, (M + 1)b_n + 1)$ to (p_n, q_n) to find a path from the origin to (p_n, q_n) above the line $Y = rX$. Since these paths have span $n = p_n + q_n$, they are also counted by $m_r(n)$. This gives the desired lower bound

$$m_r(n) \geqslant [Q(a_n, b_n)]^M, \tag{62}$$

where a_n and b_n are defined in equation (60). This result is enough to prove

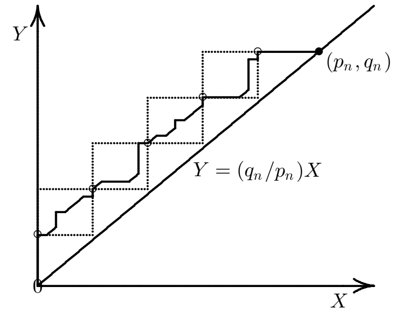

Figure 15. Paths of span $n = p_n + q_n$ can be constructed by concatenating paths crossing M rectangles of dimensions $a_n \times b_n$ where $a_n = \lfloor p_n/N \rfloor$ and $b_n = \lfloor q_n/N \rfloor$. By adding edges to join the path with the origin and with the point (p_n, q_n) the final path has span $p_n + q_n$. Since $[q_n/p_n] > r$, the path is also counted by $m_n(r)$. This gives the inequality in equation (62).

Lemma 6.5. *Let $\langle q_n/p_n \rangle$ be a sequence of rational numbers with (p_n, q_n) a pair of relative prime and positive integers. Suppose, moreover, that $[q_n/p_n] \to r$ and $[q_n/p_n] > r$, where $r > 1$ is an irrational number and that $p_n + q_n = n$ for each n. Then,*

$$\liminf_{n\to\infty} [m_r(n)]^{1/n} \geqslant Q(r)$$

where $Q(r)$ is defined in lemma 6.1.

Proof. Fix the values of a_n and b_n in equation (60) and take the power $1/n$ in equation (62). This shows that

$$[m_r(n)]^{1/n} \geqslant [Q(a_n, b_n)]^{M/(N(a_n+b_n)+v_n+u_n)},$$

where $p_n = Nb_n + v_n$ and $q_n = Na_n + u_n$. Take the lim inf on the left-hand side by taking $n \to \infty$ while keeping a_n and b_n fixed. Then $N \to \infty$ and $M \to \infty$ while $[q_n/p_n] \to r$ and $[M/N] \to 1$. Hence,

$$\liminf_{n\to\infty} [m_r(n)]^{1/n} \geqslant [Q(a_n, b_n)]^{1/(a_n+b_n)}.$$

Take $n \to \infty$ on the right-hand side. Since $[a_n/b_n] \to r$, the right-hand side approaches $Q(r)$, by lemma 6.1. □

The corollary of lemmas 6.3, 6.4 and 6.5 is

Theorem 6.6. *Suppose $r > 1$. Then,*

$$\lim_{n\to\infty} [m_r(n)]^{1/n} = Q(r) \qquad \text{for any} \quad r > 1.$$

Also observe that the paths constructed in figure 15 and leading to the inequality in equation (62) ends in the vertex (p_n, q_n). Choose $p_n = \lfloor n/2 \rfloor$ and $q_n = \lceil n/2 \rceil$, then $a_n/b_n \to 1$ in the proof of lemma 6.5. This shows that

$$\liminf_{n\to\infty} [m_{\lfloor n/2 \rfloor, \lceil n/2 \rceil}]^{1/n} \geqslant Q(1) \tag{63}$$

with the result that lemma 6.2 has corollary

Corollary 6.7. *Suppose that $r \in (0, 1)$. Then,*

$$\lim_{n\to\infty} [m_r(n)]^{1/n} = Q(1).$$

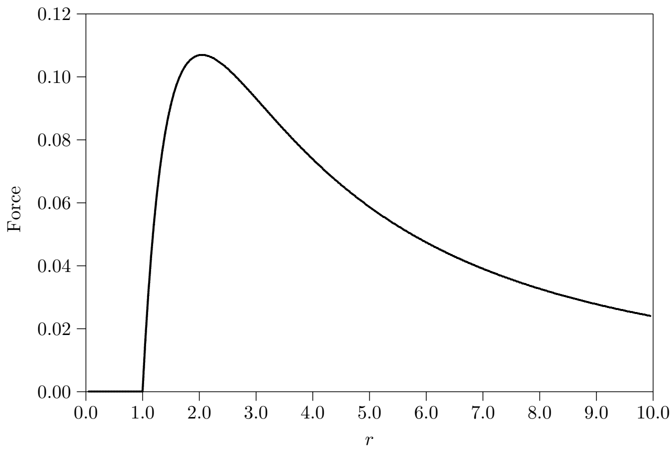

Figure 16. The magnitude of forces in r-Motzkin paths as a function of r. The curve goes through a maximum at $r = 2.0491\ldots$ where the force is $0.10704\ldots$.

Taken together, the last two corollaries determine the limit $\lim_{n\to\infty}[m_r(n)]^{1/n}$ for all positive irrational numbers. It can be extended to non-negative real numbers by defining $\lim_{n\to\infty}[m_{q/p}(n)]^{1/n} = \lim_{i\to\infty} Q(r_i)$ where $\langle r_i\rangle$ is a sequence of irrational numbers converging to q/p. In that case, the limit is equal to $Q(1)$ for any real number in [0, 1] and equal to $Q(r)$ for any real number $r > 1$. Thus,

$$\lim_{n\to\infty}[m_r(n)]^{1/n} = \begin{cases} Q(1) = 1+\sqrt{2}, & \text{if} \quad r \in (0,1), \\ Q(r), & \text{if} \quad r > 1, \end{cases} \tag{64}$$

and it is a continuous and differentiable function of r.

6.4. *Forces in NE-oriented paths*

The generating function h_r in equation (51) corresponds to a model of NE-oriented paths in an r-wedge formed by the Y-axis and the line $Y = rX$. The radius of convergence in the t-plane can be determined from equation (64):

$$t_r = \lim_{n\to\infty}[m_r(n)]^{-1/n} = \begin{cases} \dfrac{1}{1+\sqrt{2}}, & \text{if} \quad 0 \leqslant r \leqslant 1, \\ [Q(r)]^{-1}, & \text{if} \quad r > 1. \end{cases} \tag{65}$$

The limiting free energy can now be explicitly computed in this model from equation (65): with $Q(r)$ as defined in lemma 6.1,

$$\mathcal{F}(r) = \begin{cases} \log(1+\sqrt{2}), & \text{if} \quad 0 \leqslant r \leqslant 1, \\ \log Q(r), & \text{if} \quad r > 1. \end{cases} \tag{66}$$

The net entropic force in the vertical direction along the line $X = 1$ in figure 5 due to this free energy is the derivative of $\mathcal{F}(r)$ to r. This force is applied by the path on the line $Y = rX$ at the point $(1, r)$ in the negative Y-direction, forcing the wedge open, and its magnitude is plotted in figure 16.

For small $r \in [0, 1]$, the net force is identically zero, but for $r > 1$ the magnitude of the force is given by an explicit function of r. It also goes through a maximum at

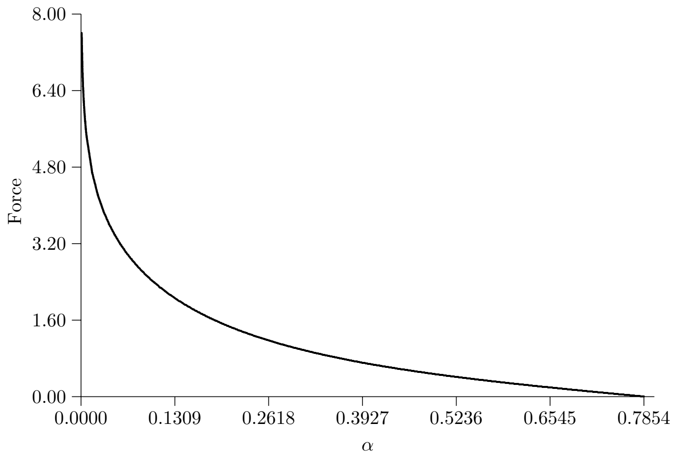

Figure 17. The magnitude of forces in r-Motzkin paths as a function of vertex angle α of the r-wedge. The curve goes to zero at $\pi/4$ and diverges logarithmically as $\alpha \to 0^+$.

$r = 2.0491\ldots$ where its magnitude is $0.107\,04\ldots$. One may expand the magnitude of the force asymptotically, this gives

$$F(r) = \frac{\log(2r)}{r^2} - \frac{1+2\log(2r)}{r^3} + O\left(\frac{\log(r)}{r^4}\right). \qquad (67)$$

Comparison with equation (49) shows that this only differs by a factor $1/2$ in the second term; this is the only effect of weighing NE-oriented edges by t^2 (as opposed by t) in this model.

The force may also be examined as a function of the vertex angle of the wedge—in this case it is directed along the normal to the line $Y = rX$ at a distance of 1 from the origin (it is the moment of the force around the origin). In figure 17, this dependence is plotted and the moment of the force diverges as a logarithm of the angle as the wedge is squeezed closed:

$$F(\alpha) = \log(2/\alpha) - \alpha(1 + 2\log(2/\alpha)) + O(\alpha^2 \log(2/\alpha)) \qquad \text{as} \quad \alpha \to 0^+. \qquad (68)$$

This result differs from equation (50) only by a factor of 2 in the subleading term. By integrating $F(r)$ the total work performed as the wedge is squeezed closed from a vertex angle larger than $\pi/4$ is obtained. The result is $0.8813735\ldots$ units of work.

7. Conclusions

In this paper, the forces and the moments of forces, exerted by an NE-oriented path confined to a wedge on the boundary of the wedge, were determined. This model is adapted from Motzkin paths, and NE-oriented paths in a wedge geometry may be considered a natural generalization of Motzkin paths.

Motzkin paths were briefly reviewed in section 2 and generalized to q-Motzkin paths in q-wedges, where q is a natural number, in section 3. In particular, I showed that the generating function of q-Motzkin paths, g_q, satisfies a $(q+1)$-degree polynomial with coefficients which are monomials in t. While a complete solution is possible for small values of q (the solution for $q = 2$ is given in section 3.1), a general solution apparently cannot be written in closed form. However, some progress can be made by examining g_q at its radius of convergence, t_q. In particular, the value of g_q at t_q, $g^* = g_q(t_q)$ satisfies a $(q+1)$-degree polynomial

$$((q-1)g^* - q)^q + (1 + q(1-g^*))^{q+1} = 0 \qquad (69)$$

and one may determine an accurate asymptotic approximation for g^*:

$$g^* = g_q(t_q) \approx 2 - \sqrt{1 - 2/q}. \tag{70}$$

The natural generalization of these models is to a model of NE-oriented paths confined in an r-wedge formed by the Y-axis and the line $Y = rX$, where $r > 0$ is irrational. The generating function is given by g_r in equation (6), and the paths are weighed by their length (defined as the total number of steps). In other words, t is the edge-generating variable in this model. In section 4, a lengthy construction resulting in corollary 4.6 determines the radius of convergence t_r of g_r. While this does not give an explicit expression for t_r, it nevertheless defines t_r in terms of the infimum of a function differentiable in a suitable subset of the real line.

The forces of the NE-oriented paths on the line $Y = rX$ are examined in section 5. The main result is lemma 5.1, and t_r can be determined by finding the roots of $(r(1-y) - y)^{r+1} - y(1-r(1-y))^r$ numerically. This is done in section 5.2, and the force and the moment of the force around the origin are plotted in figures 12 and 13. In section 5.1, the asymptotic behaviour of the force and its moment are determined, these are given in equations (49) and (50).

While the model in section 5 cannot be solved in closed form, a small change gives a model which can be solved in closed form. In section 6, NE-oriented paths in r-wedges are weighed by their span in the generating function h_r, where t is now the span-generating variable. The radius of convergence is given by t_r in equation (65), where $Q(r)$ is the explicit function defined in lemma 6.1. It is possible in principle to compute explicit expressions for the force and the moment of the force in this model.

In section 6.4 the asymptotic expansion of the force in this model is given in equation (67) and of the moment of the force in equation (68). The leading terms of these asymptotic formulae are the same as those of the first model and the subleading terms only differ by a factor of 2. Thus, the change in the model did not alter the leading term in the asymptotic expansions, and to leading order one may claim that for values of $r > 1$ and $\alpha \leqslant \pi/4$,

$$F(r) \sim \log(2r)/r^2 \qquad \text{and} \qquad F(\alpha) \sim \log(2/\alpha) \tag{71}$$

for the force and its moment in both models examined in this paper. These results coincide with the leading asymptotic terms in forces in a Dyck path model in an r-wedge [15], where it is shown that $F(r) = [\log r]/(1 + r^2)$ if $r > 1$ and $F(\alpha) \sim \log(1/\alpha)$ for $\alpha \leqslant \pi/4$. In other words, the leading behaviour of $[\log(2r)]/r^2$ and the logarithmic divergence as $\alpha \to 0^+$ appear robust in these models, and should be expected in other similarly defined models of directed paths and perhaps also even in models of partially directed paths in r-wedges.

Acknowledgment

EJJvR is supported by a grant from NSERC (Canada).

References

[1] Brak R, Essam J M and Owczarek A L 1998 New results for directed vesicles and chains near an attractive wall *J. Stat. Phys.* **93** 155–93

[2] Brak R, Owczarek A L, Rechnitzer A and Whittington S G 2005 A directed walk model of a long polymer chain in a slit with attractive walls *J. Phys. A: Math. Gen.* **38** 4309–25

[3] de Gennes P-G 1979 *Scaling Concepts in Polymer Physics* (Ithaca, NY: Cornell University Press)

[4] Duchon P 2000 On the enumeration and generation of generalized Dyck words *Discrete Math.* **225** 121–35

[5] Duplantier B and Saleur H 1986 Exact surface and wedge exponents for polymers in two dimensions *Phys. Rev. Lett.* **57** 3179–82

[6] Flory P J 1955 Statistical termodynamics of semi-flexible chain molecules *Proc. Roy. Soc.* A **234** 60–73
[7] Flory P J 1969 *Statistical Mechanics of Chain Molecules* (New York: Wiley-Interscience)
[8] Guttmann A J 2005 Self-avoiding walks in constrained and random geometries: series studies *Statistics of Linear Polymers in Disordered Media* ed B K Chakrabarti (Amsterdam: Elsevier) pp 59–101
[9] Hammersley J M 1957 Percolation processes II: the connective constant *Math. Proc. Camb. Phil. Soc.* **53** 642–5
[10] Hammersley J M and Whittington S G 1985 Self-avoiding walks in wedges *J. Phys. A: Math. Gen.* **18** 101–11
[11] Hegger R and Grassberger P 1994 Chain polymers near an adsorbing surface *J. Phys. A: Math. Gen.* **27** 4069–81
[12] Janse van Rensburg E J 2003 Statistical mechanics of directed models of polymers in the square lattice *J. Phys. A: Math. Gen.* **36** R11–61
[13] Janse van Rensburg E J 2005 Square lattice paths adsorbing on the line $Y = qX$ *J. Stat. Mech.: Theory Exp.* P09010
[14] Janse van Rensburg E J 2005 Adsorbing bargraph paths in a q-wedge *J. Phys. A: Math. Gen.* **38** 8505–25
[15] Janse van Rensburg E J and Le Y 2005 Forces in square lattice directed paths in a wedge *J. Phys A: Math. Gen.* **38** 8493–503
[16] Janse van Rensburg E J, Orlandini E, Owczarek A L, Rechnitzer A and Whittington S G 2005 Self-avoiding walks in a slab with attractive walls *J. Phys. A: Math. Gen.* submitted
[17] Napper D H 1983 *Polymeric Stabilization of Colloidal Dispersions* (London: Academic)
[18] Madras N and Slade G 1993 *The Self-Avoiding Walk* (Boston: Birkhäuser)
[19] Nienhuis B 1982 Exact critical point and critical exponents of $O(n)$ models in two dimensions *Phys. Rev. Lett.* **49** 1062–5
[20] Prellberg T and Owczarek A L 1995 Critical exponents from nonlinear functional equations for partially directed cluster models *J. Stat. Phys.* **78** 701–30
[21] Privman V, Forgacs G and Frisch H L 1988 New solvable model of polymer chain adsorption at a surface *Phys. Rev.* B **37** 9897–900
[22] Soteros C E and Whittington S G 1988 Polygons and stars in a slit geometry *J. Phys. A: Math. Gen.* **21** L857–61
[23] Whittington S G 1983 Self-avoiding walks with geometrical constraints *J. Stat. Phys.* **30** 449–56
[24] Whittington S G and Soteros C E 1991 Polymers in slabs, slits and pores *Isr. J. Chem.* **31** 127–33
[25] Whittington S G and Soteros C E 1992 Uniform branched polymers in confined geometries *Macromol. Rep.* A **29** (Suppl. 2) 195–9
[26] Vanderzande C 1998 *Lattice Models of Polymers (Cambridge Lecture Notes in Physics* vol 11*)* (Cambridge: Cambridge University Press)